

Relaxational and vibrational dynamics in the glass-transition range of a strong glass former B_2O_3

A. Brodin,* L. Börjesson, D. Engberg, and L. M. Torell

Department of Physics, Chalmers University of Technology, S-412 96 Göteborg, Sweden

A. P. Sokolov[†]

Max-Planck-Institut für Polymerforschung, D-55021 Mainz, Germany

(Received 26 May 1995)

The structural relaxation behavior of a strong glass former B_2O_3 has been investigated over broad temperature (300–1275 K) and frequency (0.5 GHz–10 THz) ranges using depolarized light scattering. The spectra clearly show nonmonotonic temperature behavior with some dynamical crossover at about $T_c \approx 800$ –900 K. Above T_c the spectra develop qualitatively according to the general scenario predicted by the mode-coupling theory (MCT), including a fast β process and a much slower α process in addition to a vibrational contribution. However, there is disagreement between the observed functional form of the fast relaxational dynamics and that predicted by MCT. The disagreement seems to be related to the influence of low-lying vibrational contributions, the so-called boson peak, which generally seems to be more pronounced in strong glass formers. Below T_c the spectra do not follow MCT predictions, not even qualitatively; the main signature is a decrease of the level of the fast relaxation spectrum. Analysis in terms of an alternative phenomenological approach, in which the fast relaxation contribution is related to the damping of the vibrational modes (giving rise to the boson peak), reveals some crossover of the damping rate at about the same temperature T_c as the crossover of the fast relaxation dynamics itself, and with similar temperature dependence as that recently reported for the Brillouin linewidth. We suggest that these variations are related to the temperature dependence of the relative strength of the fast relaxation. We show that apart from differences in the vibrational contribution, strong and fragile glass formers differ concerning the temperature range of transition (between T_c and T_g), being narrow for fragile systems ($T_c/T_g \approx 1.2$) and broad for stronger ones ($T_c/T_g \approx 1.6$ for B_2O_3).

I. INTRODUCTION

The nature of the glass transition, though much discussed and investigated through the years, is still not clear not even on a qualitative level. Glass formation is observed in a wide range of materials of quite different molecular origin, like for instance in hydrogen bonded, van der Waals, or ionic systems, or in strong covalently bonded networks. However, systems with different interatomic forces generally show different temperature behavior of the time scale τ_α of the primary relaxation, the so-called α process, which closely resembles the temperature dependence of the viscosity. The τ_α vs T plot is strongly non-Arrhenius for ionic and van der Waals liquids, weakly non-Arrhenius for hydrogen bonded systems, and nearly Arrhenius for covalently bonded structures like SiO_2 . Using the difference in temperature behavior of the α relaxation, Angell introduced a classification of glass-forming systems according to their resistance against temperature-induced structural changes.¹ In the classification the covalently bonded systems are denoted as strong, while ionic and van der Waals systems, with rapid decrease of τ_α upon increase of temperature, are denoted as fragile.

The recent development of mode-coupling theory² (MCT) for describing the structural relaxations related to the liquid-glass transition has stimulated a great number of experimental investigations of various glass formers. MCT makes both qualitative and quantitative predictions for the evolution of the relaxation spectra over the glass-transition range. Ac-

ording to MCT the relaxation decays in two steps initiated by a fast β relaxation, generally in the ps range and with a weak temperature dependence, and followed by the much slower α relaxation, which strongly varies with temperature. Moreover, according to the theory there exists a specific crossover temperature T_c , at which the thermal evolution of the dynamic spectra changes significantly.² Using some asymptotic solutions of MCT equations, the detailed behavior of the two processes, their spectral shape, interrelations, and temperature dependences were predicted.²

Experimental analysis of neutron^{3,4} and light^{5–8} scattering spectra obtained from different glass formers support the main predictions of MCT for the high-temperature ($T > T_c$) region and with a crossover temperature T_c far above the calorimetrically determined glass-transition temperature ($T_c \approx 1.2T_g$). However, so far comparisons between experimental data and the asymptotic MCT predictions have been restricted to fragile systems, which may be considered as systems of particles interacting via central forces. In the case of the relaxation dynamics of strong systems one may expect deviations from the MCT predictions, since the presence of strong directional bonds is likely to significantly influence the dynamics. In particular, it has been shown⁹ that the lowest-frequency feature in the vibrational contribution to the dynamic structure factor (the so-called boson peak) strongly increases with decrease of fragility of the system. The vibrational contribution was neglected in asymptotic solutions of MCT equations. However, it represents a signifi-

cant part of the frequency region^{10–13} where the theory predicts the presence of fast β relaxations in the spectra. In fact it is well known that below T_g there are two features in the low-frequency region (below 100 cm^{-1}) of Raman and neutron spectra of glasses which are not present in the corresponding crystalline systems: quasielastic scattering (QS) which dominates in the region below 15 cm^{-1} , and a broad band observed in the range $20\text{--}100 \text{ cm}^{-1}$, the boson peak (BP). Similar features have been observed in IR spectra of glasses.²⁶ The former contribution increases in intensity at a higher rate than the Bose population factor, as temperature is increased, and is usually attributed to some relaxation processes. It may be related to the fast β process which according to the MCT survives and can relax also in the frozen state. The latter, the boson peak which is not explicitly considered in MCT, usually follows the Bose temperature behavior, and hence represents some low-frequency vibrational excitations of the system. The physical interpretation of the boson peak is far from clear and even less known is its importance for the relaxation scenario at the liquid-glass transition. We note however that for a nonfragile system like glycerol, for which the BP is pronounced, significant deviations have recently been reported for the structural relaxation spectra from that predicted by MCT.^{14,15} It is not even clear whether in glycerol one can define a consistent crossover temperature T_c which according to MCT is expected for different parameters of the dynamical spectrum.

In the present contribution an analysis of the dynamics of a strong glass former B_2O_3 is performed over broad frequency ($0.5\text{--}10^4 \text{ GHz}$) and temperature ($T_g\text{--}2.5T_g$) ranges. The aim of the study is to investigate whether the asymptotic MCT predictions for the relaxational behavior are valid also for a strong glass former. Furthermore, we will use an alternative phenomenological approach^{10,11} to analyze the fast relaxational contribution as related to the vibrational one (the boson peak), which was neglected in MCT.

The relaxational spectra of strong glass formers present important advantages for analysis in terms of MCT, as compared to those of fragile systems, since in strong systems the fast β process is clearly separated from the α relaxation over a much wider temperature range. Even raising the temperatures to many hundreds of degrees above T_g , the α process is still too slow to significantly affect the fast response. This allows us to follow the evolution of the fast relaxation over a broad temperature range. At temperatures below $\sim 800 \text{ K}$ the relaxation spectrum of B_2O_3 has recently been analyzed using photon correlation spectroscopy (PCS).¹⁶ The PCS measurements suggest indeed a two-step relaxation behavior of the strong glass former. However, the time window of the PC technique did not allow for an investigation of the fast β relaxations in the temperature range around the suggested crossover temperature ($\sim 800 \text{ K}$) nor the fast vibrational dynamics of the boson peak and therefore the present study was undertaken.

II. EXPERIMENTAL

Samples were prepared from a B_2O_3 powder containing about 3% of water. The powder, placed in a light-scattering silica cell, was melted and kept at about 1300 K under vacuum for a period of $\sim 15 \text{ h}$, in order to obtain water-free

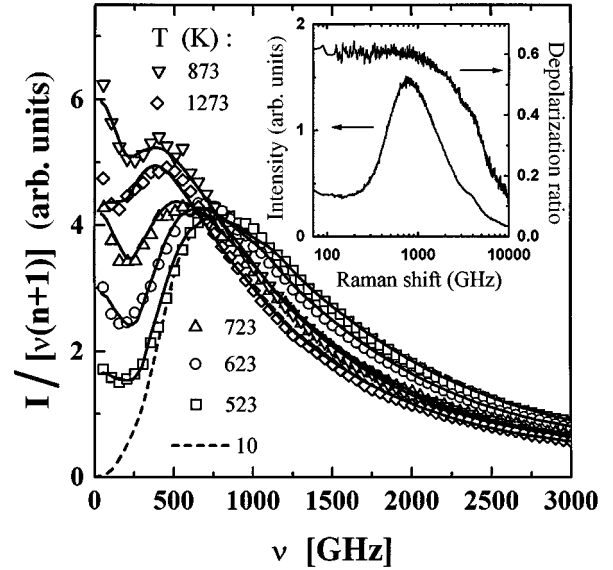


FIG. 1. Depolarized Raman spectra of B_2O_3 at various temperatures reduced by the temperature factor. Symbols represent the experimental results and solid lines represent calculated spectra [using Eq. (12)]. The dashed line represents the spectrum at $T = 10 \text{ K}$. Inset shows the polarized spectrum and the depolarization ratio ($T = 300 \text{ K}$).

samples. From analysis of the Raman OH vibration around 3600 cm^{-1} the concentration of water was estimated to be less than 0.1%. The sample was then placed in a thermostat designed for light scattering and investigated over a wide temperature range from room temperature to $\sim 1300 \text{ K}$. A low-temperature investigation at $\sim 10 \text{ K}$ was also performed. Depolarized and polarized Raman spectra were obtained at right angle scattering geometry using a double monochromator (Spex model 1403) with the spectral slit widths set to give a resolution better than 1 cm^{-1} . At higher temperatures the spectral window was extended to lower frequencies using a six-pass tandem Fabry-Perot interferometer (model Sandercocock). Depolarized spectra obtained in backscattering geometry were recorded for three different free spectral ranges (150, 35, and 7 GHz) of the interferometer. The spectra were matched to each other and to the Raman spectra. As an excitation source an Ar^+ laser was used operating at wavelength 488 nm and at power of 200 mW .

III. RESULTS

In Fig. 1 we present depolarized low-frequency Raman spectra of B_2O_3 obtained at different temperatures. The scattering has a large depolarization ratio $I_{vh}/I_{vv} \approx 0.6$ and, as can be seen in the inset in Fig. 1, it is found to be nearly constant over the frequency range from $\sim 1.5 \text{ cm}^{-1}$ ($\sim 45 \text{ GHz}$) up to the BP frequency and thereafter it decreases. The spectra in Fig. 1, presented in the Raman spectral density form $\{\text{normalized by the temperature factor } \nu[n(\nu) + 1] = \nu[1 - \exp(h\nu/kT)] - 1 \approx kT\}$, are dominated by a broad peak which is particularly pronounced in the glassy state. It is the so-called boson peak (BP) which is reported to be a general characteristic of glasses. In general, first-order Raman scattering in a disordered system reflects, in the harmonic ap-

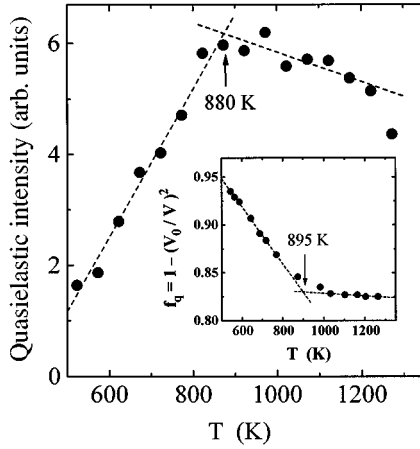


FIG. 2. Temperature dependence of the quasielastic intensity, obtained from the spectra in Fig. 1 as integrated intensity over the range 60–150 GHz. Inset shows the temperature dependence of the nonergodicity parameter as obtained from a combination of Brillouin and ultrasonic results (Refs. 29 and 35).

proximation, the vibrational density of states $g(\nu)$ weighted by the light-vibration coupling coefficient $c(\nu)$,¹⁷ i.e.,

$$I_{\text{exp}} = c(\nu)g(\nu)(n(\nu, T) + 1)/\nu. \quad (1)$$

The harmonic approximation holds at low temperatures (dashed line in Fig. 1), where all relaxations are suppressed, and here the spectrum solely represents the low-frequency harmonic (vibrational) excitations of the system, i.e., the BP. From comparisons with inelastic neutron-scattering observations for some glasses it is suggested that the BP is caused by a peculiarity in $g(\nu)$ and that $c(\nu)$ increases monotonously with increasing frequency.^{18–21}

Figure 1 demonstrates another general finding for amorphous systems,²² namely that at elevated temperatures there appears another contribution in the low-frequency spectra. Apart from the vibrational one (the boson peak), which for B_2O_3 dominates at frequencies $\nu > 300$ GHz, there is a lower-frequency contribution referred to in the literature as being relaxational or quasielastic in character,^{22–25} since in the spectral density representation it shows up as a peak centered at zero frequency. For B_2O_3 it considerably influences the spectra below 300 GHz. In the representation of Fig. 1 both contributions appear to exhibit strong temperature variations. We will see shortly, however (discussion of Fig. 3 and Sec. V), that the apparent increase of the overall intensity in Fig. 3 is mainly due to an increase of the quasielastic intensity, while the BP exhibits some softening and broadening at high temperatures. These changes are mostly pronounced as the temperature is raised from T_g (~ 525 K) up to about 850 K. As the temperature is raised further (from ~ 850 up to ~ 1275 K), the spectra stay more or less unaffected (Fig. 1) and there is even a small decrease in the quasielastic intensity. This is demonstrated in Fig. 2, which shows the temperature dependence of the quasielastic intensity, evaluated from the spectra of Fig. 1 as the integrated intensity over the frequency range 60–150 GHz, where the quasielastic contribution clearly dominates (cf. the lowest- T spectrum, where this contribution is absent). It can be seen in

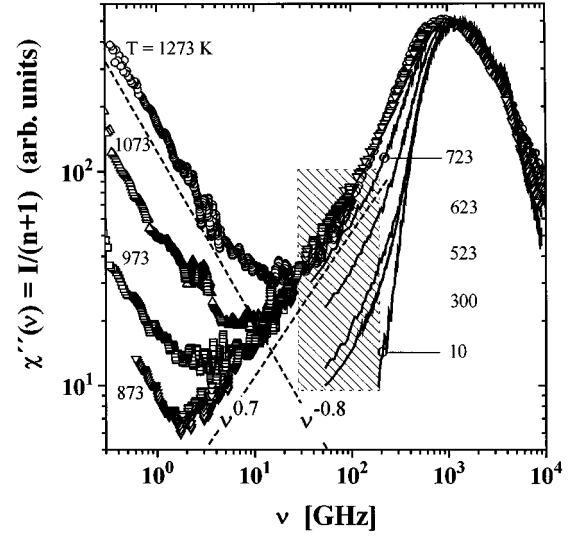


FIG. 3. Depolarized light scattering susceptibility spectra at various temperatures, scaled at the maxima. Dashed lines represent typical slopes for the α relaxation (≈ -0.8) and for the fast dynamics (≈ 0.7).

Fig. 2 that at $T \approx 900$ K there is a clear break in the temperature dependence of the quasielastic intensity.

Next we present in Fig. 3 the experimental data of Fig. 1 in the Raman susceptibility form $I_{\text{exp}}/[n(\nu, T) + 1]$. The spectra in Fig. 3 have been extended to lower frequencies by including the data obtained by the tandem Fabry-Perot technique. The data were scaled at the maximum of the susceptibility spectra around 1 THz. The susceptibility spectra allow us to analyze more easily the relaxational contribution, because a multicomponent quasielastic peak centered at zero frequency (as in the spectral density representation) will separate into a number of features peaking at different frequencies according to their different characteristic time/frequency scales. In particular, with increasing temperature the quasielastic contribution in the range 20–300 GHz is now clearly seen as growing relative to the vibrational one (cf. again the lowest- T spectrum at $T = 10$ K, which may be regarded as containing purely vibrational contribution of the BP). As the temperature is raised above ~ 800 K, we observe another feature, an upturn in the low-frequency part of the susceptibility spectra, and a minimum develops (Fig. 3). It indicates that as temperature increases a much slower relaxation process is subsequently coming into our spectral window. Hence, the susceptibility spectra exhibit three distinct contributions, separated according to their different frequency (time) scales and temperature behavior: (1) The vibrational contribution of the BP, $\nu \geq 300$ GHz, which remains harmonic (i.e., temperature independent) up to $T_g = 525$ K, though it exhibits some softening and broadening at higher temperatures (a more detailed description will be given in Sec. V). This part shall be denoted as “vibrational contribution,” or “boson peak,” throughout the paper; (2) The “quasielastic” contribution, which appears on top of the vibrational one at $\nu \leq 300$ GHz at all temperatures except for the lowest one and exhibits a strong temperature variation of its intensity. We shall denote it as “fast relaxational part of the dynamics,” or “ β -relaxation part,” since

it may be associated with the β -relaxation process of MCT, as discussed in the following section; (3) An additional relaxational contribution, which appears as an upturn on the low-frequency side of the spectra at $T > 800$ K (i.e., in the liquid state) and subsequently moves into the spectral window with raising the temperature. It will be shown to correspond to the main α -relaxation process, and accordingly it will be denoted as the “ α -relaxation,” or “slow relaxation process.”

It can be seen in Fig. 3, that in the spectral range where the fast relaxation contribution dominates, the susceptibility spectrum can be approximated by a power-law dependence $\chi''(\nu) \propto \nu^a$ with $a \approx 0.7$. This trend is most clearly seen for the 873 K spectrum, where the relevant range of frequencies spans over almost two decades. At lower temperatures, the rapidly decreasing intensity at low frequencies was not sufficient to allow for any extension of the low-frequency range by the tandem Fabry-Perot technique. However, even in these cases the lowest frequency parts of the measurable quasielastic contribution (shaded area in Fig. 3) exhibit about the same slope. This is true even for $T = 300$ K, i.e., deep into the glassy state. Thus, the exponent a appears to be essentially temperature independent and the main variation is the change of the quasielastic intensity. It can be seen in Fig. 3 that also the slow relaxation process can be approximated by a power law $\chi''(\nu) \propto \nu^{-b}$, in this case with an exponent $b \approx 0.8$. This value is close to that obtained for the α process from photon-correlation spectroscopy,¹⁶ and the width of the relaxation spectrum is also in close correspondence with that of the log-Gaussian distribution used to fit ultrasonic measurements of the α relaxation.²⁷

IV. ANALYSIS OF THE RELAXATION PATTERN IN THE FRAMEWORK OF MCT

A. The MCT scenario for the dynamics of the glass transition

Before the analysis of the light-scattering data we briefly summarize the main predictions of MCT.² MCT describes the time evolution of the density-density correlation function $F_q(t)$ after the “transient” (ps time) evolution has passed, and predicts a two-step relaxation decay. At short times it is initiated by a fast relaxation and $F_q(t)$ decreases to some finite value $f_q(t) < 1$ which is temperature dependent. Thereafter, for temperatures above some critical temperature T_c a much slower process, the primary α relaxation, proceeds and $F_q(t)$ decays from $f_q(t)$ to zero. The temperature behavior of f_q is expected to show critical behavior at the temperature T_c according to

$$\begin{aligned} f_q(T) &= f_0 + 0(T), \quad T > T_c \\ &= f_0 + h\sqrt{T_c - T}, \quad T < T_c, \end{aligned} \quad (2)$$

where $0(T)$ is a slowly changing function. Thus, different scenarios are predicted for the spectra at temperatures above and below T_c (we are considering only the idealized version of MCT, which is sufficient for the present analysis). Around T_c some asymptotic solutions for MCT equations have been found.² In the frequency domain they predict that the high-frequency tail of the α relaxation is represented by a non-Debye form in the susceptibility spectra $\chi''(\nu)$ which asymp-

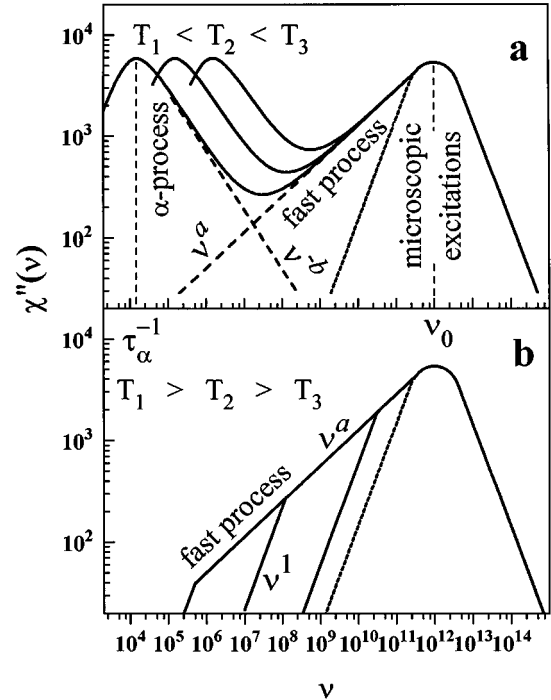


FIG. 4. Qualitative scenario predicted by MCT for the temperature evolution of the susceptibility spectra at $T > T_c$ (a) and $T < T_c$ (b).

totically follows a power-law dependence $\chi''(\nu) \propto \nu^{-b}$. The low-frequency tail of the fast relaxation should, according to MCT, follow another power-law dependence $\chi''(\nu) \propto \nu^a$. At still higher frequencies this part merges with the “microscopic excitation band” [Fig. 4(a)], which is supposed to include all the “transient” dynamics of the system. The functional form of the latter is not considered by the MCT, the only assumption being that its frequency/time scale is well separated from that of both slow and fast relaxational dynamics.

At high temperatures ($T > T_c$) the spectrum of the fast relaxation is predicted to be essentially temperature independent whereas the characteristic time scale τ_α of the α relaxation varies rapidly with temperature at unchanged spectral shape and amplitude² [Fig. 4(a)]. As a result the minimum in the susceptibility spectra between the α relaxation and the fast process is expected to have a universal form (the master curve) which is well approximated by an interpolation formula of two power laws [Fig. 4(a)]:

$$\chi''(\nu) = \chi_{\min} \{ b(\nu/\nu_{\min})^a + a(\nu/\nu_{\min})^{-b} \} / (a+b). \quad (3)$$

Here χ_{\min} denotes the value of the susceptibility at the minimum between the α and the fast relaxations and ν_{\min} is the corresponding frequency of the minimum. The temperature dependences of the minimum parameters χ_{\min} and ν_{\min} are predicted to be interrelated such that

$$\chi_{\min} \propto (\nu_{\min})^a. \quad (4)$$

Moreover, they are expected to be linked to the temperature variation of the α -relaxation time scale by the following relations:

$$\chi_{\min} \propto (\tau_{\alpha})^{-ab/(a+b)}, \quad (5a)$$

$$\nu_{\min} \propto (\tau_{\alpha})^{-b/(a+b)}. \quad (5b)$$

Furthermore, MCT predicts a critical temperature behavior of τ_{α} at temperatures above the critical temperature T_c according to

$$\tau_{\alpha} \propto (T - T_c)^{-\gamma}. \quad (6)$$

As a consequence also χ_{\min} and ν_{\min} are expected to display critical temperature behavior. In asymptotic MCT predictions all three exponents a , b , and γ should be interrelated by the equations

$$\gamma = 1/2(a+b) \quad (7a)$$

and

$$\Gamma^2(1-a)/\Gamma(1-2a) = \Gamma^2(1+b)/\Gamma(1+2b), \quad 0 < b < 1, \quad 0 < a < 0.395, \quad (7b)$$

where $\Gamma(x)$ is the gamma function.

At the critical temperature T_c , MCT predicts a dynamical crossover from liquidlike to solidlike behavior. In this sense T_c corresponds to some kind of ideal glass-transition temperature. Below T_c MCT describes a different scenario for the temperature evolution of the susceptibility spectrum [Fig. 4(b)]. Then the α relaxation becomes fully arrested (in the idealized version) and the fast relaxation spectrum shows a significant temperature variation. The fast relaxation is present above a certain frequency ν_{β} below which the spectrum only contains a white-noise contribution with linear frequency dependence. As a result a crossover, or ‘‘knee,’’ appears in the spectra at ν_{β} and it is expected to shift to higher frequency with decreasing temperature. It leads to the temperature dependence of the nonergodicity parameter $f_q(T)$ [Eq. (2)], i.e., the strength of the β relaxation decreases with decreasing temperature.

Summarizing this part, we would like to stress that the MCT predictions presented above are asymptotic solutions of MCT equations around the critical temperature T_c and also that the vibrational contribution was assumed to be negligible in the spectral window of interest.²

B. Analysis of the spectra at high temperatures

Let us start our analysis with a few remarks about the light-scattering mechanism. In depolarized light scattering one measures anisotropy fluctuations, while MCT describes density-density fluctuations. The relation between these two quantities is not clear. However, comparisons of light- and neutron-scattering spectra, which so far has been performed for Ca-K-NO₃ (CKN) and glycerol,¹⁵ show that around the susceptibility minimum both spectra are almost identical. Thus, it was suggested that one can analyze the light-scattering susceptibility spectrum $\chi''(\nu) = I(\nu)/(n+1)$ in the framework of MCT. This approach has already been used in the analysis of the light-scattering data obtained for several fragile and intermediate glass formers^{5-8,14,15} and it will be used in the present work.

Without any data treatment one can clearly see a correspondence between the susceptibility spectra of B₂O₃ for

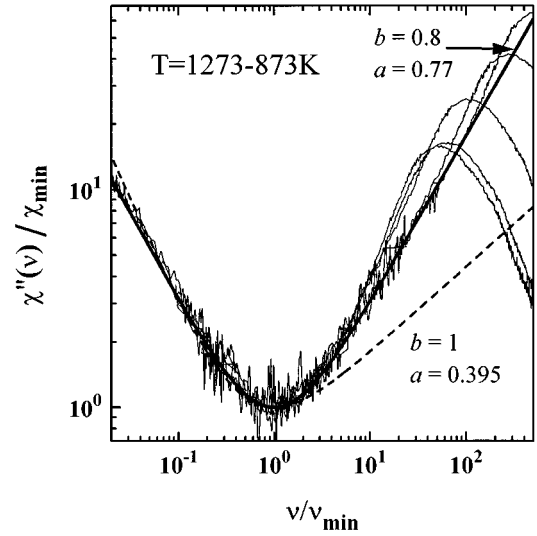


FIG. 5. Master curve for the susceptibility minimum constructed from susceptibility spectra obtained at various temperatures and shifted so that their minima overlap. Solid line represents a fit of Eq. (3) with free exponents a and b . Dashed line represents a fit with the exponents a and b related through the MCT restriction [Eq. (7b)].

$T > 850$ K (Fig. 3) and the schematic picture of MCT for the high-temperature range $T > T_c$ [Fig. 4(a)]: the spectrum of fast dynamics is essentially temperature independent and the main temperature variation is the shift of the α -relaxation tail into the experimental frequency window. As a consequence, one can construct a master curve of the susceptibility minimum by shifting the spectra in a log-log plot such that their minima overlap (see Fig. 5). The individual curves fall on a common master curve, which shows that the shape of the relaxation spectrum around the susceptibility minimum is temperature independent, within the experimental accuracy. This is in agreement with the MCT. An approximation of the master curve by the sum of the two power laws [Eq. (3)] with exponents a and b fixed through the MCT relation [Eq. (7b)] cannot, however, describe the experimental results; a fit that gives reasonable agreement on the low-frequency side of the minimum ($b=1$, $a=0.395$) leads to a strong deviation on the high-frequency side (see dashed line Fig. 5). Ignoring the restriction of a and b [Eq. (7b)] then the minimum can be well approximated by Eq. (3) with $a \approx 0.77$ and $b \approx 0.8$ (Fig. 5). The latter values of the exponents do not obey the predicted interrelation [Eq. (7b)] and, furthermore, the value of a is significantly higher than the limiting value ($a=0.395$) of MCT.

Another test of the MCT predictions can be performed by analyzing the data of χ_{\min} and ν_{\min} according to Eqs. (4) and (5). Figure 6(a) shows the observed values of χ_{\min} and ν_{\min} for various temperatures. As can be seen the data set in Fig. 6(a) follows a power law with exponent $a=0.64$ [Eq. (4)], which is once again much higher than the limiting value predicted by MCT, but is in reasonable agreement with that obtained from the master curve (Fig. 5). In Fig. 6(b) we show the data of χ_{\min} and ν_{\min} plotted vs $(\tau_{\alpha})^{-1}$ in order to test Eqs. (5a) and (5b). Values of τ_{α} were estimated from viscosity data²⁸ using the Stokes-Einstein relation $\tau_{\alpha} \sim \eta/T$.

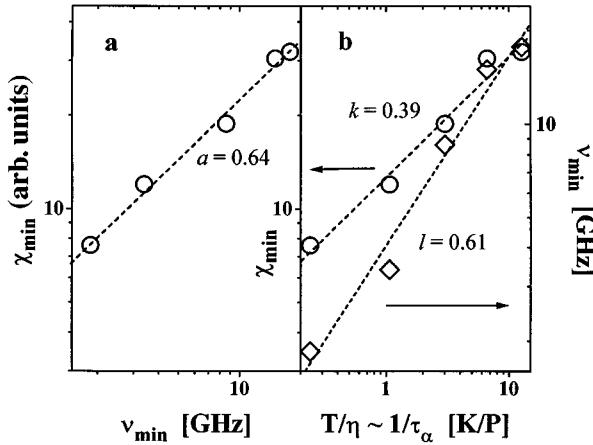


FIG. 6. Crosstest of the temperature behavior of the minimum parameters χ_{\min} , ν_{\min} , and for the α relaxation time scale τ_{α} [Eqs. (4), (5)]. (a) χ_{\min} vs ν_{\min} ; (b) χ_{\min} (\circ) and ν_{\min} (\diamond) vs T/η . Slopes of lines fitted to the data are given in the figure.

The exponents k and l obtained from Fig. 6(b) lead to $a=0.64$ and $b=1.0$, which are in a reasonable agreement with the values of a and b obtained from a free fit of the master curve. The fact that a master curve can be constructed and that the spectra and their minima parameters scale with the viscosity [shown by the results in Fig. 6(b)] shows that the data for $T > 800$ K support an MCT-like qualitative scenario: the spectra are a superposition of a constant fast dynamics and a slow α relaxation, the latter moves on the frequency scale following the temperature dependence of the viscosity, however keeping its shape and amplitude. The deviation appears in the slope of the fast relaxation, which in the case of B_2O_3 is much larger than the asymptotic MCT predictions [Eqs. (7)].

C. Crossover temperature T_c and the dynamics below T_c

MCT predicts critical divergence of the viscosity and the α relaxation when approaching T_c from higher temperatures. However, as found for other glassformers, the temperature dependence of the viscosity (or τ_{α}) does not show divergence at any temperature in the range of interest. Still one may use Eq. (6) for analysis of the viscosity time scale in the high-temperature region and in this way locate T_c of MCT. This was done for B_2O_3 in Refs. 16 and 29 using an exponent of $\gamma \approx 2.1-2.4$ corresponding to a b value in the range 0.65–0.8 and the critical temperature was then estimated to $T_c \approx 800-900$ K.

According to MCT there should be other changes in the dynamics of glass-forming liquids at T_c , e.g., the spectrum of fast dynamics should be independent of temperature above T_c and become temperature dependent at $T < T_c$ (see Fig. 4). The data presented in Figs. 1, 2, and 3 clearly show that there is some significant change in the temperature behavior of the Raman spectra in the range $T \approx 800-900$ K; the intensity of the quasielastic spectrum strongly varies at lower temperatures and becomes nearly temperature independent above 850 K (Fig. 2). Extrapolating the two temperature dependences in Fig. 2 we estimate a crossover temperature at

about $T_c \approx 880$ K. It is interesting to note that the crossover occurs not only well above T_g ($T_c/T_g \approx 1.6$), but also above the melting point $T_m = 723$ K.

Let us now turn to the analysis of the susceptibility spectrum below T_c (Fig. 3). Within our experimental frequency window ($\nu > 50$ GHz) no sign of any ‘‘knee’’ has been found in the investigated temperature range. The spectral shape of the fast relaxation [$\chi''(\nu) \propto \nu^{0.7}$] is nearly temperature independent, whereas the intensity decreases strongly with decreasing temperature. The decrease is not related to the shift of the knee, as predicted by MCT [see Fig. 4(b)]. Thus, at $T < T_c$ there is a marked deviation from the MCT scenario even on a qualitative level.

V. QUASIELASTIC INTENSITY AND THE BOSON PEAK SPECTRUM

We note from the preceding section that the behavior of the high-frequency dynamics is not well described by MCT. In the following we will therefore take an alternative approach and analyze the spectral behavior in the higher-frequency window ≥ 100 GHz with the aim of also including the boson peak in the interpretation of the behavior of the fast dynamics.

A useful characteristic of the low-frequency Raman scattering of glasses is its depolarization ratio. It has been analyzed for many glass-forming systems and found to vary from ~ 0.24 for ZBLAN20 and ~ 0.3 for SiO_2 up to values close to 0.75 (the maximum possible value for isotropic systems) for several organic, ionic, and van der Waals systems.^{5,10,22,30} An important finding, which holds in all the mentioned cases, is that the depolarization ratio is the same for both the quasielastic scattering and the boson peak, and that it is essentially independent of temperature. This is also the case for B_2O_3 , see inset in Fig. 1, where the depolarization ratio vs frequency is presented. It can be seen in Fig. 1 that the value of 0.6 is unchanged on passing from 100 GHz (where the spectral intensity is dominated by the QS) up to 1000 GHz (which marks the maximum of the BP). It is therefore likely that the origin of the QS is related to the vibrational dynamics.³¹ It has been suggested^{22,31} that the deviations of the glass network from strictly harmonic behavior can be described by replacing Ω^2 by $\Omega^2 + M(\Omega, \nu)$ for the vibrational mode Ω , in the Raman susceptibility function;

$$\chi(\Omega, \nu) = \frac{C(\Omega)}{\nu^2 - [\Omega^2 + M(\Omega, \nu)]}, \quad (8)$$

where $C(\Omega)$ is the light-to-vibration coupling function. $M(\Omega, \nu)$ may be regarded as a ‘‘memory function.’’ A possible mechanism behind Eq. (8) is that relaxation processes supported by a disordered structure (e.g., relaxations of two-level systems, relaxing anharmonic soft potential sites, etc.) act as a random force upon the harmonic modes, and the latter perceive it as a viscous-like damping. We would like to stress that general form for the susceptibility function [Eq. (8)] is similar with starting MCT equations. However, in its asymptotic predictions [Eqs. (3)–(7), which are traditionally used for analysis of the experimental data] MCT neglects the vibrational contribution and focuses on the long-time, low-

frequency tails of the memory function $M(\Omega, \nu)$. In our approach we will focus mainly on the vibrational part assuming some simple behavior for the memory function.

The specific memory function, if considered phenomenologically, can be defined from the observed spectra behavior. Since we have found the spectral *shape* of the relaxational contribution to be nearly independent of temperature, we assume that only the *magnitude* of $M(\Omega, \nu)$ has a strong temperature dependence. We further assume the relaxational contribution to be weak such that the vibrations constituting the BP remain well-defined excitations at all temperatures, as discussed above, i.e., $|M| \ll \Omega^2$. We can then rewrite Eq. (8) as

$$\chi(\Omega, \nu) = \frac{C(\Omega)}{\nu^2 - \Omega^2 [1 + g(T)m(\Omega, \nu)]}, \quad (9)$$

where $|m| < 1$, and $g(T) \ll 1$ determines the temperature-dependent strength. The quantity deduced from Raman scattering (Fig. 3) is proportional to the sum, taken over all the vibrational modes of the BP:

$$\chi''(\nu) = \sum_i \chi''(\Omega_i, \nu). \quad (10)$$

In the limit $T \rightarrow 0$ [and hence $g(T) \rightarrow 0$] the susceptibility is given by the limiting value $\chi_0''(\nu)$ of a harmonic oscillator:

$$\chi_0''(\Omega, \nu) = \text{Im} \frac{C(\Omega)}{\nu^2 - \Omega^2 - i0} = \frac{\pi}{2} \frac{C(\Omega) \delta(\nu - \Omega)}{\Omega}, \quad (11a)$$

$$\sum_i \chi_0''(\Omega_i, \nu) = \chi_0''(\nu). \quad (11b)$$

By combining Eqs. (9), (10), and (11), we obtain

$$\chi''(\nu) = \text{Im} \frac{2}{\pi} \int_{\Omega} \frac{\Omega \chi_0''(\Omega)}{\nu^2 - \Omega^2 [1 + g(T)m(\Omega, \nu)]} d\Omega, \quad (12)$$

where $\chi_0''(\nu)$ can be taken from the spectrum at low enough temperatures such that all relaxations are suppressed. For comparisons with experimental data a relevant memory function $m(\Omega, \nu)$ needs to be chosen. A single exponential relaxation seems adequate in the present case since the spectrum of $\chi''(\nu)$ vs ν on the log-log scale exhibits a slope ~ 0.7 in the range of the quasielastic scattering, see Fig. 3, which is not too far from the appropriate value of unity. Thus, following the model,³¹ we use $m = -i\nu\tau/(1 - i\nu\tau)$ and Eq. (12) to fit the experimental spectra. $g(T)$ is taken as a free fit parameter as is also τ . We also varied the boson peak maximum frequency to account for the mentioned softening, as only a part of the experimentally observed softening is accounted for in Eq. (12). Thus, the phenomenological model adopted appears to be very similar to that used in Refs. 10 and 11 for the same purpose and can describe the Raman spectra reasonably well (Fig. 1). The so obtained τ is found to be only slightly temperature dependent, which is in accordance with our previous observation of a temperature-independent spectral shape of the QS. The controlling parameter g is analogous to the relative intensities of the Rayleigh and Brillouin peaks, known as the Landau-Placzek ratio in hydrodynamic models, and measures, in the limit

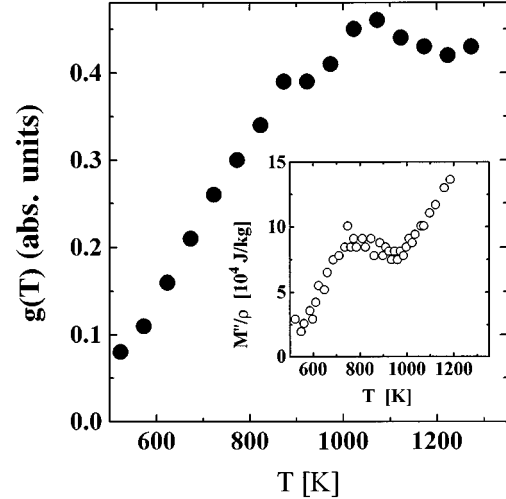


FIG. 7. Temperature dependence of the damping parameter for the boson peak vibrations obtained from fits of Eq. (12) to the low-frequency Raman data (see Fig. 1). Inset shows data for the Brillouin-line damping (Ref. 32).

$g(T) \ll 1$, the ratio of the integral intensities of the relaxational and vibrational contribution to the Raman spectral density in Fig. 1. The obtained temperature dependence of $g(T)$ is demonstrated in Fig. 7 and it is found to be similar to that of Fig. 2, which also reflects the relaxation strength.

The results of Fig. 7 demonstrate again two temperature regions with a crossover at $T \sim 800$ – 900 K; the relaxation strength (and thus the BP damping) increases almost linearly with temperature up to 800 K, and then is essentially temperature independent. It is instructive to compare these results with those for the Brillouin linewidth $\Delta\nu_B$ recently reported for B_2O_3 by Kieffer.³² The temperature dependence of the imaginary part of the elastic modulus $M''/\rho \approx \Delta\nu_B \cdot \nu_B$ (ν_B is the Brillouin frequency) exhibits a maximum just at $T \sim 800$ K (see inset in Fig. 7), which cannot be related to the main α -relaxation process. The α process is too slow to influence the Brillouin modes at these temperatures (see for example Fig. 3), and only provides a contribution to $\Delta\nu_B$ at much higher temperatures ($T > 1000$ K, see inset in Fig. 7). We want to stress the similarity of the temperature variation of the BP damping and that of the Brillouin lines, which may be due to that the two processes couple to the same relaxation mechanism.

VI. DISCUSSION

During recent year MCT has been shown to successfully describe neutron- and light-scattering data for a range of fragile glass formers. Even quantitatively the detailed asymptotic [Eqs. (2)–(7)] MCT predictions have been verified, at least for high temperatures ($T > T_c$).^{3–8} Of nonfragile systems only a few have so far been analyzed according to MCT, namely B_2O_3 (Ref. 16) and glycerol.^{14,15} In the case of the former system photon correlation spectroscopy (PCS) shows a two-step relaxation time decay in accordance with the MCT predictions though the measurements were done below the critical temperature T_c of the theory. In the case of glycerol, again both fast and slow relaxations were observed,

though quantitative disagreement with the asymptotic MCT predictions for the master curve was found. The value of the a exponent was in the case of glycerol estimated to $a \approx 1$, which is much larger than that accepted from the theory.

In the present study of B_2O_3 we extend the previous long-time/low-frequency PCS investigation to much higher frequencies using combined Fabry-Perot interferometer and Raman spectrometer techniques. In B_2O_3 , which can be regarded as a strong glass former, the fast β process is well resolved from the slower a process over a much broader temperature range than for the fragile ones. At higher temperatures, $T > 850$ K, the spectra clearly demonstrate similarity with the qualitative picture predicted by MCT for the high ($T > T_c$) temperature region [Fig. 4(a)]: the spectrum of fast dynamics (including the fast β relaxation and the boson peak) is essentially temperature independent and the main change of the spectrum is due to the a relaxation which moves into the detected frequency window as the temperature is raised. Plotting the master curve for the susceptibility minimum (Fig. 5) the predicted relations between the minimum parameters and τ_α were found to be in reasonable agreement with the experimental results (Fig. 6). Thus the relaxation scenario of the strong glass former B_2O_3 follows in the high-temperature region qualitatively that predicted by MCT.

However, trying to apply asymptotic MCT predictions for a quantitative description of the evolution of the spectra of B_2O_3 , the analysis fails, especially concerning the fast β relaxations. The exponent $a \approx 0.77$ of the β process is too high (Fig. 5), as was also previously reported in the case of the relaxation data for glycerol.^{14,15} Deviations from the MCT predicted spectral shape can moreover be found in the case of fragile liquids and again noted on the high-frequency side of the master curve (see analysis presented in Ref. 33). The value of the a parameter obtained from the fit of the minimum parameters [Eq. (5)] is for all liquids analyzed so far (CKN,⁵ salol,⁶ orthoterphenyl (OTP),⁸ and glycerol^{14,15}) significantly higher than the value calculated from the master curve using the constraints of the MCT relation [Eq. (7b)]. As was shown in Ref. 33 this deviation is small for extremely fragile CKN, more pronounced for the less fragile systems OTP, salol, and *m*-tricresyl phosphate (*m*-TCP), and still more pronounced for nonfragile glycerol. Thus one can tentatively conclude that the spectrum of fast dynamics generally deviates from that predicted by asymptotic MCT solutions and that the deviation increases as the fragility of the system decreases. The effect may be related to the contribution of the boson peak vibrations, which were neglected by MCT. In particular we note that the strength of the boson peak is reported to increase with decrease of the degree of fragility.⁹

Another important prediction of MCT is the crossover temperature T_c at which the relaxation dynamics is expected to change character with critical temperature behavior for some parameters of the relaxation spectrum [Eqs. (5) and (6)]. For experimentally investigated glass formers there is no critical behavior observed for the α -relaxation time scale around T_c , not even for the extremely fragile systems, and this problem has been dealt with in the extended version of MCT (Refs. 2 and 34) by introducing some additional hopping process. However, crossover in the relaxation dynamics

has been observed at a specific temperature T_c for a range of fragile systems with T_c typically 50–100 °C above the calorimetrically determined glass-transition temperature T_g . For B_2O_3 a crossover in the dynamics clearly shows up at $T \approx 800$ –900 K. It appears in the temperature dependence of the quasielastic intensity (Fig. 2) determined from the integrated low-frequency Raman intensity. It has also been reported for the same temperature range from an analysis of hypersonic velocities²⁹ and likewise from the intensity of elastic neutron scattering³⁵ in accordance with MCT predictions. We also note that there is a crossover in the damping rate of the boson peak (Fig. 7) and in the recent data for the Brillouin linewidth³² (see inset Fig. 7).

We further note that the crossover temperature for B_2O_3 is not only above T_g ($T_c/T_g \approx 1.6$), but also above the melting point ($T_m \approx 725$ K). For fragile systems T_c is generally noted closer to T_g ($T_c/T_g \approx 1.2$), though it has been suggested¹¹ that the T_c/T_g ratio increases with decrease of the fragility of the system in accordance with the present observation for B_2O_3 . Thus, while the temperature range of the glass transition (temperature interval between T_g and T_c) is short for fragile glass formers it is extremely broad for B_2O_3 . Indeed, previous Brillouin observations of transverse modes indicate that the covalent network structure of B_2O_3 survives even at temperatures above T_m .

While above T_c the dynamic spectra of B_2O_3 qualitatively follow the scenario predicted by MCT, there is no agreement in the temperature range below the crossover temperature [$T < 850$ K, Fig. 4(b)], not even on a qualitative level. There is no sign of any ‘‘knee’’ in the spectral shape of the fast dynamics as suggested by the MCT but rather a strong decrease of the quasielastic scattering intensities keeping the shape unchanged (Fig. 3). Also, as temperature decreases the boson peak becomes increasingly more pronounced (Fig. 1). Thus, one can speculate upon whether the observed temperature variations of the fast relaxation dynamics (Fig. 2) is related to the change of the boson peak rather than being related to the strength of the α process as suggested in the MCT.

According to the model of damped oscillators^{10,11,31} an increase of the fast relaxation process intensity is related to an increased damping of the boson peak. Using this model the Raman spectra of OTP, *m*-TCP, and glycerol have been analyzed and the boson peak vibrations were found to become overdamped at temperatures around the crossover T_c as estimated from MCT analysis.¹¹ The present results show that this is not the case for B_2O_3 ; the boson peak is clearly observed in the Raman spectra at $T \approx T_c$ and even above (Fig. 1), and the damping rate $g(T)$ is significantly smaller than 1 (Fig. 7). We note however, that the temperature dependence of the damping rate changes just at the crossover temperature T_c (Fig. 7).

We also note that the temperature dependence of the boson peak ‘‘damping’’ parameter $g(T)$ behaves in a similar way as the recently reported damping parameter of the Brillouin lines. In the measurements of the Brillouin linewidths of B_2O_3 a maximum was noted at around $T \sim 800$ K (see inset in Fig. 7), which cannot be related to the main α -relaxation process. The behavior of the Brillouin lines was interpreted by Kieffer³² using a traditional hydrodynamic approach, assuming two additional relaxation processes apart

from the α relaxation. The maximum in the Brillouin linewidth then appears when the condition for maximum damping of the sound waves is fulfilled, i.e., for $2\pi\nu_B\tau \approx 1$ (τ is a characteristic time scale for the relaxation and, ν_B is the Brillouin frequency). Assuming activated temperature dependence for the relaxation time $\tau = \tau_0 \exp(-E/kT)$, the temperature of the maximum for any frequency ν may be estimated.

However, the light-scattering spectra (Fig. 3) does not show any relaxation process coming through the Brillouin frequency window ($\sim 15\text{--}20$ GHz) at around 800 K. There is only variation of the quasielastic intensity for the fast relaxation and only at higher temperatures does the tail of the α relaxation reach the Brillouin frequency window (the latter leads to the observed increase of the Brillouin linewidth at $T > 1000$ K, inset Fig. 7). We also note that the temperature dependence of the damping parameter for the Brillouin lines, as likewise that of the boson peak, follows the behavior of the quasielastic intensity (Fig. 2). This similarity may be explained by that the two phenomena couple to the same fast β process and that the variation of the damping is related to the change of the overall intensity of the fast relaxation rather than to the relaxation time of a particular relaxation process becomes comparable with $(2\pi\nu)^{-1}$. Since the intensity of the fast relaxation process varies with temperature in a similar way at all frequencies (including the frequency of the Brillouin peak ν_B , and that of the boson peak ν_{\max}), the corresponding damping parameters are expected to have similar temperature dependences as is actually observed.

VII. CONCLUSIONS

The presented analysis of the depolarized light-scattering spectra of B_2O_3 clearly shows that the structural relaxation dynamics of the strong glass former has a nonmonotonic temperature dependence. There is a different behavior at high and low temperatures with a crossover observed at about $T_c \approx 800\text{--}900$ K. Above T_c the qualitative scenario predicted by the mode coupling theory describes the experimental data well. However, there is significant quantitative

disagreement with the asymptotic MCT predictions similar to what has been reported previously for glycerol,^{14,15} another nonfragile glass former. It is apparent in the spectrum of fast dynamics which deviates from the MCT functional form and may be related to the pronounced vibrational contributions (the boson peak) typical of strong glass formers.

Below T_c the behavior of the dynamic spectra does not follow the MCT scenario not even on a qualitative level: there is a decrease of the quasielastic scattering intensity without any essential change of its spectral form, the so-called “knee” is absent, and there is the development of the boson peak. The behavior of the fast dynamics in the temperature region below T_c may be related to a smooth change from relaxational-type molecular motions (liquidlike behavior) to vibrational ones (solidlike behavior). A significant difference between B_2O_3 and fragile glass formers is the temperature range between T_c and T_g which is much wider for the strong system.

Another striking observation is the similarity of the temperature dependence of the damping parameters of the boson peak vibrations in the THz range and that reported for the acoustic vibrations at Brillouin frequencies ($\sim 15\text{--}20$ GHz). Moreover, the temperature behavior of the two vibrational damping parameters is similar to that of the quasielastic scattering intensity of the fast relaxation. The damping cannot be explained in the framework of a traditional hydrodynamic approach and it is suggested that the damping rate varies due to the temperature variation of the intensity of the fast process.

ACKNOWLEDGMENTS

This work has been supported by the Swedish Natural Science Research Council. The assistance of Dr. A. A. Sokolov in the data analysis of the boson peak spectra is appreciated. A.P.S. is grateful to the Max-Planck-Gesellschaft for financial support, to the Royal Swedish Academy of Sciences for a research grant, and to Chalmers University of Technology for hospitality. A.P.S. also appreciates the partial financial support from INTAS and ISF.

*Permanent address: Institute of Semiconductors Physics, Nation. Acad. Sci., 252650 Kiev, Ukraine.

†Permanent address: IA&E Russian Academy of Sci., 630090 Novosibirsk, Russia.

¹C. A. Angell, in *Relaxation in Complex Systems*, edited by K. L. Ngai and G. B. Wright (Office Naval Research, Washington, D.C., 1984), p. 3.

²W. Götze and L. Sjögren, *Rep. Prog. Phys.* **55**, 241 (1992).

³See, for instance, in *Dynamics of Disordered Materials*, edited by D. Richter, A. J. Dianoux, W. Petry, and D. Teixeira (Springer, Berlin, 1989) and *Dynamics of Disordered Materials II*, edited by A. J. Dianoux, W. Petry, and D. Richter (North-Holland, Netherlands, 1993).

⁴W. Knaak, F. Mezei, and B. Farago, *Europhys. Lett.* **7**, 529 (1988).

⁵G. Li, W. M. Du, X. K. Chen, H. Z. Cummins, and N. J. Tao, *Phys. Rev. A* **45**, 3867 (1992).

⁶G. Li, W. M. Du, A. Sakai, and H. Z. Cummins, *Phys. Rev. A* **46**, 3343 (1992).

⁷W. M. Du, G. Li, H. Z. Cummins, M. Fuchs, J. Toulouse, and L. A. Knauss, *Phys. Rev. E* **49**, 2192 (1994).

⁸W. Steffen, A. Patkowski, H. Gläser, G. Meier, and E. W. Fischer, *Phys. Rev. E* **49**, 2992 (1994).

⁹A. P. Sokolov, E. Rössler, A. Kisliuk, and D. Quitman, *Phys. Rev. Lett.* **71**, 2062 (1993).

¹⁰V. Z. Gochiyayev, V. K. Malinovsky, V. N. Novikov, and A. P. Sokolov, *Philos. Mag. B* **63**, 777 (1991).

¹¹A. P. Sokolov, A. Kisliuk, D. Quitman, A. Kudlik, and E. Rössler, *J. Non-Cryst. Solids* **172-174**, 138 (1994).

¹²V. K. Malinovsky and V. N. Novikov, *J. Phys. Condens. Matter* **4**, L139 (1992).

¹³B. Frick and D. Richter, *Phys. Rev. B* **47**, 14 795 (1993).

¹⁴E. Rössler, A. P. Sokolov, A. Kisliuk, and D. Quitmann, *Phys. Rev. B* **49**, 14 967 (1994).

¹⁵J. Wuttke, J. Hernandez, G. Li, G. Coddens, H. Z. Cummins, F. Fujara, W. Petry, and H. Sillescu, *Phys. Rev. Lett.* **72**, 3052 (1994).

- ¹⁶D. Sidebottom, R. Bergman, L. Börjesson, and L. M. Torell, Phys. Rev. Lett. **71**, 2260 (1993).
- ¹⁷R. Shuker and R. W. Gammon, Phys. Rev. Lett. **4**, 222 (1970).
- ¹⁸A. Fontana, F. Rocca, M. P. Fontana, B. Rosi, and A. J. Dianoux, Phys. Rev. B **41**, 3778 (1990).
- ¹⁹V. K. Malinovsky, V. N. Novikov, P. P. Parshin, A. P. Sokolov, and M. G. Zemlyanov, Europhys. Lett. **11**, 43 (1990).
- ²⁰U. Buchenau, M. Prager, N. Nüker, A. J. Dianoux, N. Ahmad, and W. A. Phillips, Phys. Rev. B **34**, 5665 (1986).
- ²¹T. Achibad, A. Boukenter, and E. Duval, J. Chem. Phys. **99**, 2046 (1993).
- ²²J. Jackle, in *Amorphous Solids: Low-Temperature Properties*, edited by W. A. Phillips (Springer, Berlin, 1981), p. 135.
- ²³V. L. Gurevich, D. A. Parshin, J. Pelous, and H. R. Schober, Phys. Rev. B **48**, 16 318 (1993).
- ²⁴G. Carini, M. Federico, A. Fontana, and G. A. Saunders, Phys. Rev. B **47**, 3005 (1993).
- ²⁵A. Brodin, A. Fontana, L. Börjesson, G. Carini, and L. M. Torell, Phys. Rev. Lett. **73**, 2067 (1994).
- ²⁶U. Strom and P. C. Taylor, Phys. Rev. B **16**, 5512 (1977).
- ²⁷P. B. Macedo and T. A. Litovitz, Phys. Chem. Glasses **6**, 69 (1965).
- ²⁸P. B. Macedo, W. Capps, and T. A. Litovitz, J. Chem. Phys. **44**, 3357 (1966).
- ²⁹L. M. Torell, L. Börjesson, A. P. Sokolov, Transp. Theory Stat. Phys. **24**, 1097 (1995).
- ³⁰J. Schroeder, S. Saha, M. Silvestri, M. Lee, and C. Moynihan, J. Non-Cryst. Solids **161**, 173 (1993).
- ³¹G. Winterling, Phys. Rev. B **12**, 2432 (1975).
- ³²J. Kieffer, Phys. Rev. B **50**, 17 (1994).
- ³³A. P. Sokolov, W. Steffen, and E. Rössler, Phys. Rev. E **52**, 5105 (1995).
- ³⁴H. Z. Cummins *et al.*, Phys. Rev. E **47**, 4223 (1993).
- ³⁵D. Engberg, L. Börjesson, J. Swenson, L. M. Torell, and W. S. Howells (unpublished).